Nanoscale local structures of rhombohedral symmetry in the orthorhombic and tetragonal phases of $BaTiO_3$ studied by convergent-beam electron diffraction

Kenji Tsuda,* Rikiya Sano, and Michiyoshi Tanaka

Institute of Multidisciplinary Research for Advanced Materials, Tohoku University, 2-1-1, Katahira, Aoba-ku, Sendai 980-8577, Japan

(Received 30 July 2012; revised manuscript received 25 November 2012; published 17 December 2012)

The symmetries of the rhombohedral, orthorhombic, and tetragonal phases of barium titanate ($BaTiO_3$) are investigated using convergent-beam electron diffraction. Nanometer-sized local structures with rhombohedral symmetry are observed in both the orthorhombic and tetragonal phases. This indicates that an order-disorder character exists in phase transformations of $BaTiO_3$. The nanostructures in these phases are discussed in terms of an order-disorder model with off-centered Ti in the ⟨111⟩ directions.

DOI: 10.1103/PhysRevB.86.214106 PACS number(s): 77.80.B−, 61.05.J−, 68.37.Lp

I. INTRODUCTION

Barium titanate ($BaTiO_3$) is a well-known ferroelectric material that undergoes structural phase transformations from a high-temperature paraelectric cubic phase to three low-temperature ferroelectric phases with tetragonal, orthorhombic, and rhombohedral symmetries. Despite extensive studies over the decades, the mechanism of these transitions—in particular their order-disorder character versus their displacive character—remains a matter of discussion. Displacive-type transitions are considered to occur in $BaTiO_3$, which are described by the condensation of a soft phonon mode,[1] and a soft mode in the cubic phase has been observed by means of neutron inelastic scattering,[2,3] although the soft mode was strongly overdamped. On the other hand, the existence of an order-disorder character has been reported as the result of a number of experiments and theories, such as x-ray diffuse scattering,[4,5] electron paramagnetic resonance (EPR),[6,7] nuclear magnetic resonance (NMR),[8,9] extended x-ray absorption fine structure (EXAFS) and x-ray absorption near edge structure (XANES),[10] pulsed x-ray laser,[11] second harmonic generation,[12] eight-sight model,[13] Landau-Devonshire theory,[14] and first-principles Monte Carlo simulations.[15] The coexistence of displacive and order-disorder characters has been examined with a microscopic model.[16] An order-disorder model of phase transformations with off-centering of Ti in the ⟨111⟩ directions was proposed by Takahasi[13] and Comes *et al.*[4] They considered that nanometer-sized structures with off-centered Ti randomly exist in the cubic phase. Comes *et al.*[4] assumed nanostructures with one-dimensional chain structures to interpret x-ray diffuse scattering sheets in the cubic, tetragonal, and orthorhombic phases. However, Harada *et al.* reported that the diffuse scattering sheets in the cubic and tetragonal phases are dynamically caused by low-frequency transverse optical phonon modes,[17,18] and a low-frequency mode at the cubic phase was confirmed from inelastic neutron scattering experiments.[2] Local structures related to an order-disorder character have been observed neither in crystal structure analyses using neutron and x-ray diffraction nor by TEM to date.[19–21]

Convergent-beam electron diffraction (CBED) has become established as the most powerful technique for determining crystal symmetries of specimen areas of a few nanometers in diameter because of the nanometer-sized electron probe used and the strong dynamical-diffraction (multiple-diffraction) effect.[22,23] In this study, the CBED method is applied to examine the symmetries of the local structures of the three ferroelectric phases of $BaTiO_3$. The results of the CBED experiments reveal an order-disorder character for the phase transformations and are discussed using an order-disorder model with off-centered Ti.[13]

II. EXPERIMENTAL

Single crystals of $BaTiO_3$ used in this study were produced by the top-seeded solution growth (TSSG) method at Fujikura Ltd. Specimens for transmission electron microscopy were prepared by crushing the single crystals and dispersing the fragments onto microgrids for electron microscopy. The CBED experiments were conducted using a JEM-2010FEF transmission electron microscope (TEM) equipped with a field emission electron gun and an in-column Omega-type energy filter.[24,25] A liquid-nitrogen-cooling specimen holder was used for cooling the specimens. Mesoscopic-scale ferroelectric domains were observed in TEM images. Energy-filtered CBED patterns were obtained from defect-free single domain areas of about 1 nanometer in diameter at an accelerating voltage of 100 kV with an acceptance energy width of 10 eV. The thicknesses of the specimen areas examined by CBED were 50–100 nanometers. CBED patterns were taken with a slow-scan CCD camera. The exposure time of the CBED patterns was set to 2 s. Crystal orientations were determined from the positions of higher order Laue zone reflections of the CBED patterns, which are not shown in the figures.

$BaTiO_3$ has a perovskite-type crystal structure. The relations between the axes of the rhombohedral, orthorhombic, and tetragonal phases and their pseudocubic axes are expressed by $\mathbf{a}_{\mathrm{tet}} = \mathbf{a}_{\mathrm{pc}}^{(\mathrm{tet})}$, $\mathbf{b}_{\mathrm{tet}} = \mathbf{b}_{\mathrm{pc}}^{(\mathrm{tet})}$, $\mathbf{c}_{\mathrm{tet}} = \mathbf{c}_{\mathrm{pc}}^{(\mathrm{tet})}$, $\mathbf{a}_{\mathrm{orth}} = \mathbf{a}_{\mathrm{pc}}^{(\mathrm{orth})}$, $(\mathbf{b}_{\mathrm{orth}} + \mathbf{c}_{\mathrm{orth}})/2 = \mathbf{b}_{\mathrm{pc}}^{(\mathrm{orth})}$, $(-\mathbf{b}_{\mathrm{orth}} + \mathbf{c}_{\mathrm{orth}})/2 = \mathbf{c}_{\mathrm{pc}}^{(\mathrm{orth})}$, $\mathbf{a}_{\mathrm{rhom}} = \mathbf{a}_{\mathrm{pc}}^{(\mathrm{rhom})}$, $\mathbf{b}_{\mathrm{rhom}} = \mathbf{b}_{\mathrm{pc}}^{(\mathrm{rhom})}$, $\mathbf{c}_{\mathrm{rhom}} = \mathbf{c}_{\mathrm{pc}}^{(\mathrm{rhom})}$, where subscript pc means pseudocubic axes. Hereafter, these pseudocubic axes are used to express the zone axis directions and reflection indices.

III. RESULTS AND DISCUSSION

Figure 1 shows a CBED pattern of the rhombohedral phase taken at approximately 90 K with the $[100]_{\mathrm{pc}}$ $(=[100]_{\mathrm{rhom}})$ zone-axis incidence. A difference map between the original and mirror-operated patterns $\Delta I/I$ is attached with a color presentation, where the mirror is indicated by the yellow line in the figure. In the difference pattern, the outside and peripheral

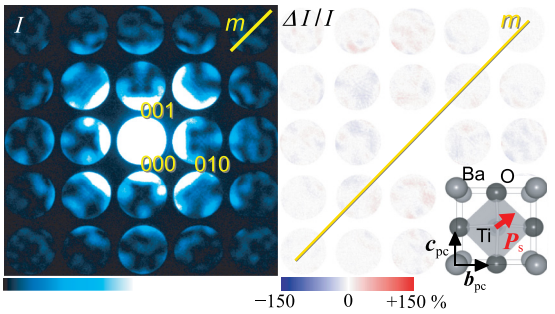

FIG. 1. (Color online) CBED pattern of the rhombohedral phase of $BaTiO_3$ taken at 90 K with the $[100]_{pc}$ (=$[100]_{rhom}$) incidence. Difference map between original and mirror-operated patterns $\Delta I/I$ is attached with a color presentation, where the mirror is indicated by a yellow line. Corresponding projected structure is shown as an inset, the projected direction of ferroelectric polarization being indicated by a red arrow.

areas of the CBED disks were masked. The corresponding projected structure is schematically shown as an inset with the projected direction of ferroelectric polarization (red arrow). The CBED pattern of the zeroth-order Laue zone (ZOLZ) reflections reveals the symmetry of the structure projected along the incident beam direction. The CBED pattern of Fig. 1 exhibits a mirror symmetry parallel to the polarization direction, which is consistent with the space group $R3m$ of the rhombohedral phase. The difference map confirms the mirror symmetry because only a small difference is seen.

The mirror symmetry can be also confirmed from a difference index of $S = \sqrt{\sum \Delta I_i^2 / \sum I_i^2}$, where ΔI_i and I_i are the difference intensity and original intensity of the ith pixel of the pattern. The S value is calculated to be 11.1% for the CBED pattern of Fig. 1, which is comparable to that of about 10% for silicon.[26] From the CBED patterns taken by step scanning of the electron probe in 5–10 nanometer steps, it was confirmed that all the specimen areas examined show one clear mirror symmetry of the rhombohedral phase. The three mirror symmetries of the rhombohedral space group $R3m$ were confirmed from CBED patterns taken from different domains connected by 71° or 109° walls.

Figures 2(a) and 2(b) show CBED patterns of the orthorhombic phase taken at approximately 200 K with the $[001]_{pc}$ (=$[0\bar{1}1]_{orth}$) and $[100]_{pc}$ (=$[100]_{orth}$) incidences, respectively. Difference maps between original and mirror-operated patterns are attached, where the mirror operations are indicated in the figures. As indicated by the yellow arrowheads, the $[001]_{pc}$ pattern of Fig. 2(a) shows a breakdown of the mirror symmetry parallel to the polarization. The difference map clearly shows the breakdown with significant intensity differences. The value of the difference index S was 30.1% for the pattern of Fig. 2(a), which is much larger than that of Fig. 1. Note that this symmetry indicated by a yellow dotted line is expected from the space group $Amm2$ of the orthorhombic phase. The symmetry breaking cannot be attributed to lattice strains and lattice defects because the correct symmetry was observed at the same areas in the rhombohedral phase. This observation indicates that nanometer-scale local structures or domains exist that do not belong to the space group $Amm2$ in the orthorhombic phase, but belong to a lower symmetry.

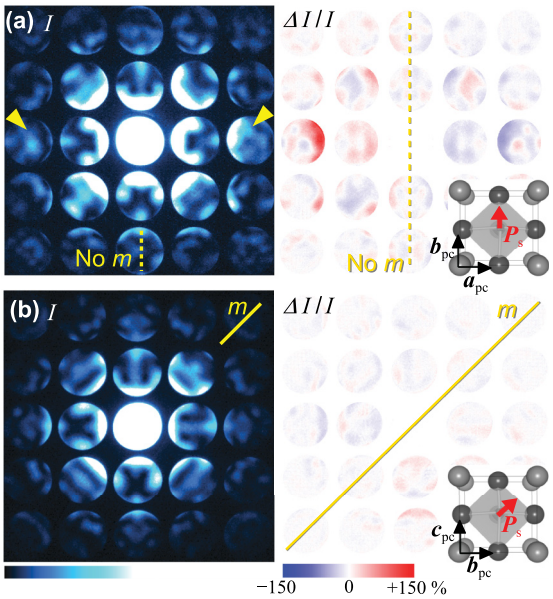

FIG. 2. (Color online) CBED patterns of the orthorhombic phase of $BaTiO_3$ taken at 200 K with (a) the $[001]_{pc}$ (=$[0\bar{1}1]_{orth}$) incidence and (b) the $[100]_{pc}$ (=$[100]_{orth}$) incidence, respectively. Difference maps with respect to the mirror symmetries indicated by the dotted and solid lines are attached, where the projected structures are shown as insets.

From the viewpoint of the successive phase transformations, it is considered that the nanoscale local structure takes the structure of the rhombohedral symmetry of the lowest temperature phase, though the possibility of a monoclinic symmetry cannot be negated in theory. However, it should be noted that the pattern of Fig. 2(a) does not also have a mirror symmetry parallel to the $[110]_{pc}$ and $[1\bar{1}0]_{pc}$ of the rhombohedral phase. If we assume that the illuminated area contains clusters with rhombohedral symmetry of different orientations, the loss of both the mirror symmetries is reasonably interpreted.

The $[100]_{pc}$ CBED pattern of Fig. 2(b) shows a mirror symmetry parallel to the polarization. This result or the conservation of the symmetry is understandable, even if nanostructures with rhombohedral symmetry of different orientations coexist in the illuminated volume, because this mirror symmetry is common to both the orientations.

Figure 3(a) shows a CBED pattern of the tetragonal phase taken at room temperature with the $[001]_{pc}$ (=$[001]_{tet}$) incidence, where the mirror symmetries expected from the space group $P4mm$ of the tetragonal phase are denoted by yellow dotted lines. As indicated by yellow arrowheads, all these mirror symmetries are broken. The attached difference map shows a clear breakdown of the mirror indicated in the figure. It should be noted that the breaking of the mirror symmetry along the $[110]_{pc}$ direction is relatively small. This implies that the clusters with the rhombohedral symmetry of one orientation are dominant in the illuminated area. If clusters with orthorhombic symmetry coexist with clusters of tetragonal symmetry in the illuminated area, mirror symmetry along $[100]_{pc}$ or $[010]_{pc}$ should remain. Thus, no orthorhombic nanostructures exist because the mirror symmetry is not seen

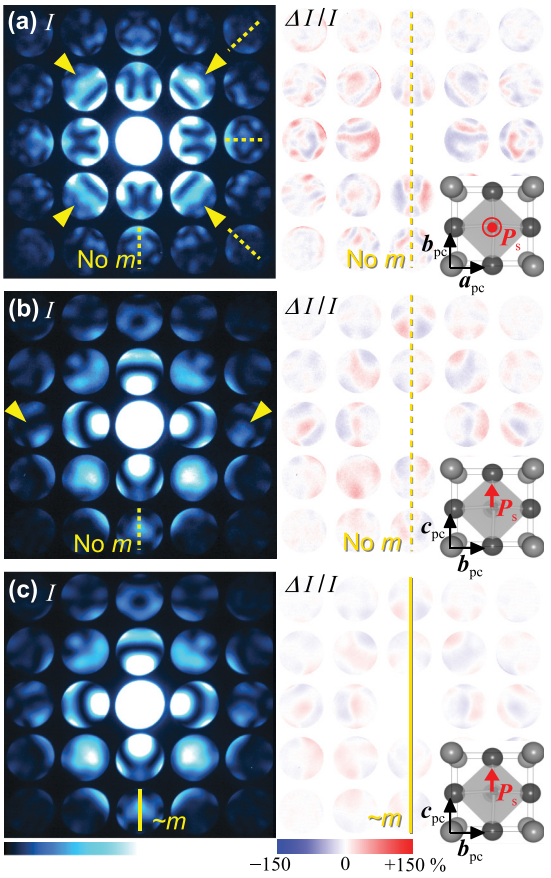

FIG. 3. (Color online) CBED patterns of the tetragonal phase of $BaTiO_3$ taken at room temperature with (a) the $[001]_{pc}$ (=$[001]_{tet}$) incidence and (b) & (c) the $[100]_{pc}$ (=$[100]_{tet}$) incidence, respectively. Pattern (c) shows a $[100]_{pc}$ pattern averaged over 25 patterns taken each from an area of 5 nm in diameter. Difference maps with respect to the mirror symmetries indicated are attached, where the projected structures are shown as insets.

in Fig. 3(a). The $[100]_{pc}$ CBED pattern of Fig. 3(b) show the breaking of the mirror symmetry along the $[001]_{pc}$ direction, which is indicated by a yellow dotted line and is expected from the tetragonal phase. The attached difference map also confirms the breaking of the mirror symmetry or breaking of tetragonal symmetry indicated in the figure. This is consistently explained only by the coexistence of nanostructures with rhombohedral symmetry of different orientations in the illuminated area.

It was found that symmetry and intensity distribution of the CBED patterns change from place to place in a nanometer scale. The pattern changed in all directions without any anisotropic feature. Figure 3(c) shows a $[100]_{pc}$ CBED pattern averaged over the 25 CBED patterns taken from areas approximately 5 nm in diameter, together with its difference map of the mirror symmetry indicated by the yellow line. The breaking of mirror symmetry clearly seen in Fig. 3(b) is reduced in the averaged pattern of Fig. 3(c). This indicates that rhombohedral local structures with a size of the order of nanometers exist in the four allowed orientations in the tetragonal phase. It is considered that several local structures are contained in the direction of the incident beam because the specimen thicknesses are 50–100 nm. The CBED pattern shows the averaged symmetry of the nanostructures contained in the beam direction. If only one variant of the rhombohedral nanostructures is dominant in the thickness direction, the CBED pattern does not show the averaged symmetry but nearly rhombohedral symmetry. Thus, the symmetry breaking cannot be observed by conventional x-ray and neutron diffraction experiments because the sizes of the examined areas are much larger than nanometers. The symmetry breaking can only be observed by a CBED experiment using a nanometer-sized electron probe.

The symmetry breaking discovered in the orthorhombic and tetragonal phases in this study can be explained not by a model of the displacive-type structural phase transformation but by a model of an order-disorder character. Let us interpret the symmetries of the observed CBED patterns in terms of the model used for the order-disorder transition of the electric polarizations of $BaTiO_3$ proposed by Takahasi.[13] Figure 4 shows schematic diagrams of the model of the off-centering of the Ti atoms in the ⟨111⟩ directions, along which electric polarization appears.

Figure 4(a) shows a model of the rhombohedral phase. It has no disorders because there is only one position (blue spot) for the off-centered Ti. Note that eight variants of the different off-centered Ti positions form macroscopic domains of the rhombohedral phase. Figure 4(b) shows a model of the orthorhombic phase. It has two possible positions (shown by two blue spots) for the off-centered Ti. This means that local structures take rhombohedral symmetry with two variants, which are incompatible with the space group *Amm*2 of the orthorhombic phase. The macroscopic polarization $\mathbf{P}_s^{avr}$ in the $[011]_{pc}$ (=$[001]_{orth}$) direction of the orthorhombic phase appears as the mean or averaged direction of the two

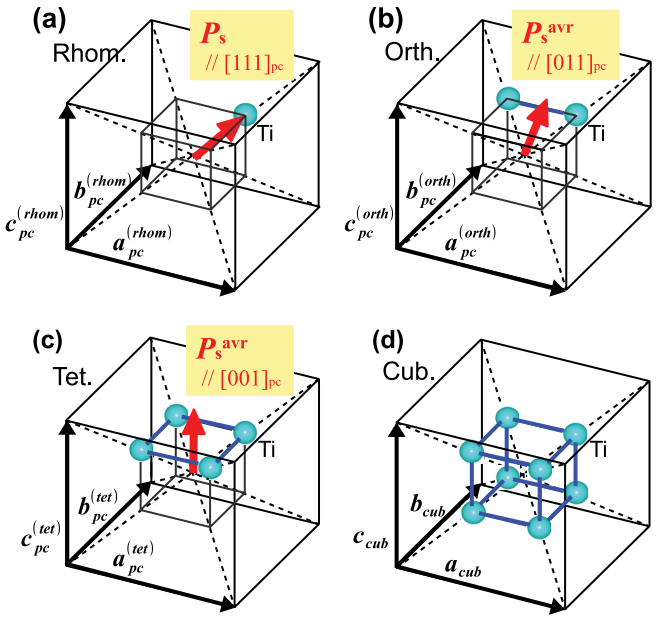

FIG. 4. (Color online) Schematic diagrams of the model of Ti off-centering in ⟨111⟩ directions (Ref. 13). Models of (a) the rhombohedral phase, (b) the orthorhombic phase, (c) the tetragonal phase, and (d) the cubic phase.

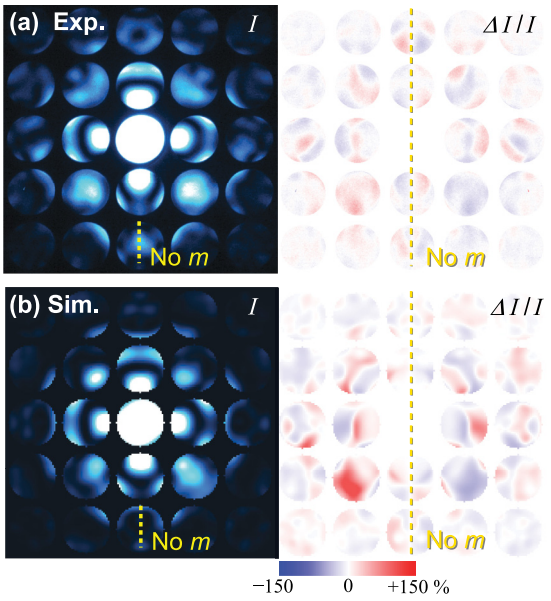

FIG. 5. (Color online) (a) Experimental and (b) simulated CBED patterns of the tetragonal phase of $BaTiO_3$. Difference maps with respect to mirror symmetries indicated are attached.

polarization directions ($[111]_{pc} + [\bar{1}11]_{pc} = [011]_{pc}$). From Fig. 4(b), it is expected that the symmetry of a local structure different from that of an averaged structure can be observed in the $[001]_{pc}$ incident beam direction, but not at the $[100]_{pc}$ direction. However, if an illuminated volume contains variants of the rhombohedral symmetry, CBED patterns of the $[001]_{pc}$ incidence do not show even the mirror symmetry of the rhombohedral symmetry. This corresponds well with the symmetries of the observed CBED patterns of Figs. 2(a) and 2(b). Figure 4(c) shows a model of the tetragonal phase. It has four possible positions for the off-centered Ti, again indicating the existence of four variants of local structures with rhombohedral symmetry, which violates the space group $P4mm$ of the tetragonal phase. The macroscopic polarization $\mathbf{P}_s^{avr}$ in the $[001]_{pc}$ (=$[001]_{tet}$) of the tetragonal phase appears as the averaged direction of the four polarization directions. The symmetry of the local structure, which is different from that of the averaged structure, can be observed for both $[100]_{pc}$ and $[001]_{pc}$ incident beam directions. Similarly to the case of the orthorhombic phase, if an illuminated volume contains variants of the rhombohedral symmetry, CBED patterns of the $[100]_{pc}$ and $[001]_{pc}$ incidences do not show the mirror symmetry of the rhombohedral symmetry. This is consistent with the symmetries of the observed CBED patterns of Figs. 3(a) and 3(b).

If we accept the order-disorder model of Fig. 4, a local structure always takes a rhombohedral symmetry, and orthorhombic and tetragonal symmetries are created by a random mixing of the different variants of rhombohedral structures. Figure 4(d) shows a model of the cubic phase, which has eight possible sites for the off-centered Ti. Thus, CBED patterns taken with {100} incidences at the cubic phase are expected to show symmetry breaking caused by the local structures of rhombohedral symmetry. However, if the temperature is increased, Ti atoms will dynamically take the eight positions due to the thermal energy. Then, it may be difficult to observe the symmetry breaking by CBED.

To estimate the magnitude of Ti displacement, CBED patterns were simulated with changing the amount of Ti displacement by the dynamical diffraction theory. Here the specimen volume for the simulation is assumed to be uniform, although the actual volume may consist of several clusters. Figure 5 shows an experimental $[100]_{pc}$ CBED pattern of the tetragonal phase (a) and a simulated pattern from a model with a Ti displacement of 0.13 Å (b). The clear breaking of the mirror symmetry is seen in the simulated pattern. The simulated pattern (b) is seen to some extent to reproduce the experimental pattern (a). It is noted that such a small displacement cannot be observed even with recent aberration-corrected TEM and scanning transmission electron microscopy (STEM) imaging techniques.

As for the directions of Ti off-centering, the present result is consistent with those of x-ray diffuse scattering[4] and EXAFS and XANES,[10] but not with EPR[7] and NMR,[8,9] which indicated Ti off-centering in ⟨100⟩ directions. This is possibly attributed to their different time scales of experimental probes.

IV. CONCLUDING REMARKS

Nanometer-sized local structures with rhombohedral symmetry were directly observed in the orthorhombic and tetragonal phases of $BaTiO_3$ using CBED in this study. This result has revealed the existence of an order-disorder character in the orthorhombic and tetragonal phases of $BaTiO_3$. The nanometer-sized structures discovered in this study are static, not dynamic, because the recorded CBED patterns are taken by integrating diffraction signals over an exposure time of 2 s. This study demonstrates that the CBED method using a nanometer electron probe is a powerful tool for investigating nanometer-scale local structures in phase transformations. The result shows no indication of the existence of chain structures as proposed by Comes *et al.*[4] An investigation of the size and shape of a nanostructures with rhombohedral symmetry in the orthorhombic and tetragonal phases is currently underway through the combined use of STEM and CBED techniques. CBED experiments for the cubic phase are planned to reveal an order-disorder character in the ferroelectric-paraelectric phase transformation. Quantitative structure analysis using CBED, which was developed by Tsuda *et al.*,[25,27,28] is also promising for determining all the atom positions of the local structures and whether the off-centering of Ti atoms is in the ⟨111⟩ directions or in other directions.

ACKNOWLEDGMENTS

The authors are grateful to T. Hashimoto, Nihon University, for providing single-crystal $BaTiO_3$. The authors thank M. Terauchi for his helpful discussion and encouragement, and F. Satou and M. Ageishi for their careful maintenance of the JEM-2010FEF. This study was partially supported by a Grant-in-Aid for Scientific Research (B) (No. 20340070) from the Ministry of Education, Culture, Sports, Science, and Technology of Japan.

*k_tsuda@tagen.tohoku.ac.jp

[1]W. Cochran, Adv. Phys. **9**, 387 (1960).
[2]G. Shirane, B. C. Frazer, V. J. Minkiewicz, J. A. Leake, and A. Linz, Phys. Rev. Lett. **19**, 234 (1967).
[3]J. Harada, J. D. Axe, and G. Shirane, Phys. Rev. B **4**, 155 (1971).
[4]R. Comes, M. Lambert, and A. Guinier, Solid State Commun. **6**, 715 (1968).
[5]R. Comes, M. Lambert, and A. Guinier, Acta Cryst. A **26**, 244 (1970).
[6]K. A. Müller and W. Berlinger, Phys. Rev. B **34**, 6130 (1986).
[7]G. Völkel and K. A. Müller, Phys. Rev. B **76**, 094105 (2007).
[8]B. Zalar, V. V. Laguta, and R. Blinc, Phys. Rev. Lett. **90**, 037601 (2003).
[9]B. Zalar, A. Lebar, J. Seliger, R. Blinc, V. V. Laguta, and M. Itoh, Phys. Rev. B **71**, 064107 (2005).
[10]B. Ravel, E. A. Stern, R. I. Vedrinski, and V. Kraizman, Ferroelectrics **206-207**, 407 (1998).
[11]K. Namikawa, M. Kishimoto, K. Nasu, E. Matsushita, R. Z. Tai, K. Sukegawa, H. Yamatani, H. Hasegawa, M. Nishikino, M. Tanaka, and K. Nagashima, Phys. Rev. Lett. **103**, 197401 (2009).
[12]A. M. Pugachev, V. I. Kovalevskii, N. V. Surovtsev, S. Kojima, S. A. Prosandeev, I. P. Raevski, and S. I. Raevskaya, Phys. Rev. Lett. **108**, 247601 (2012).
[13]H. Takahasi, J. Phys. Soc. Jpn. **16**, 1685 (1961).
[14]S. Chaves, F. C. S. Barreto, R. A. Nogueira, and B. Zeks, Phys. Rev. B **13**, 207 (1976).
[15]W. Zhong, D. Vanderbilt, and K. M. Rabe, Phys. Rev. Lett. **73**, 1861 (1994).
[16]R. Pirc and R. Blinc, Phys. Rev. B **70**, 134107 (2004).
[17]J. Harada, M. Watanabe, S. Kodera, and G. Honjo, J. Phys. Soc. Jpn. **20**, 630 (1965).
[18]J. Harada and G. Honjo, J. Phys. Soc. Jpn. **22**, 45 (1967).
[19]T. P. J. Harada and Z. Barnea, Acta Cryst. A **26**, 336 (1970).
[20]R. H. Buttner and E. N. Maslen, Acta Cryst. B **48**, 764 (1992).
[21]G. H. Kwei, A. C. Lawson, S. J. L. Billinge, and S.-W. Cheong, J. Phys. Chem. **97**, 2368 (1993).
[22]M. Tanaka, in *International Table for Crystallography*, 3rd ed., edited by U. Shumueli, Vol. B (International Union of Crystallography, Springer, 2008), p. 307.
[23]M. Tanaka and K. Tsuda, J. Electron Microsc. **60**(suppl. 1), S245 (2011).
[24]M. Tanaka, K. Tsuda, M. Terauchi, K. Tsuno, T. Kaneyama, T. Honda, and M. Ishida, J. Microsc. **194**, 219 (1999).
[25]K. Tsuda and M. Tanaka, Acta Cryst. A **55**, 939 (1999).
[26]M. Tanaka, M. Terauchi, and K. Tsuda, *Convergent-Beam Electron Diffraction III* (JEOL-Maruzen, 1994).
[27]K. Tsuda, K. Takagi, Y. Ogata, T. Hashimoto, and M. Tanaka, Acta Cryst. A **58**, 514 (2002).
[28]Y. Ogata, K. Tsuda, and M. Tanaka, Acta Cryst. A **64**, 587 (2008).